ЭППТ 2015

ACED 2015

1.1. COMPUTATION OF NONLINEAR MAGNETIC FUNCTIONS IN ELECTROMAGNETIC BRAKES FOR ELECTRIC DRIVE SYSTEMS

Johannes Steinbrunn
Faculty of Electrical and Computer Engineering,
University of Applied Sciences, D-87435 Kempten, Germany
Phone +49 831-25230, E-mail: josteinbrunn@hotmail.com

Abstract: This paper describes the computation of magnetic quantities as magnetic flux, flux density, field intensity, magnetic force, etc. in the magnetic circuit of spring operated electromagnetic brakes which are applied to rotary motions of drives as for elevators, tool machines, robots, and many other applications. The linear approach which is usually applied to determining magnetic functions gives unsatisfying results because the magnetic material of the brake is operated deeply in the saturation. The development of a nonlinear simulation model which avoids the big tool with finite elements by using numeric iterations and the method of co-energy yields results that are close to values gained via measurements. Hence, the developed method can be applied for further technical improvements of the brake's performance.
Keywords: Electromagnetic brake, armature, magnetic flux, magnetic force, simulation software, mechatronics

1. Introduction

An electromagnetic brake is an essential part of any drive system, and it serves for bringing the rotary or linear motion of the drive components to a complete and safe stand still within a short time period, particularly in an emergency case. The design of the investigated spring operated brake with its different mechanical and electrical components is shown in Figure 1. A rotationally symmetric design for the air gap is preferred to keep leakage fields and curl fields small [1].

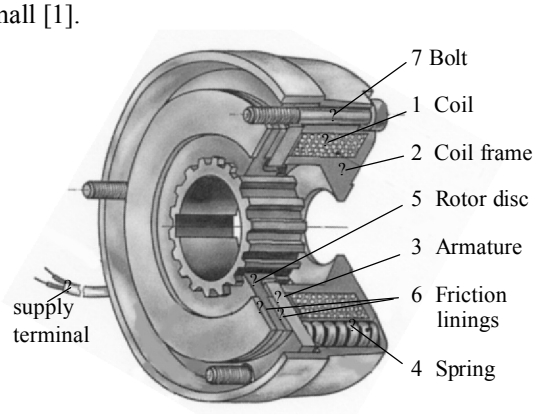

Figure 1: Design of the electromagnetic brake

The coil (1) with the coil frame (2) is the electromagnetic part of the brake. The armature (3) cannot rotate due to fixing bolts (7) but moves in axial direction by sliding along the bolts. Compression springs (4) push the armature against the rotor disc (5) with friction linings (6) on both surfaces which are then pressed against the armature and bottom plate. When the armature hits the friction disc, the braking operation is initiated.
The spring and magnetic forces act in axial direction. If the current in the coil produces a magnetic force higher than the spring force and friction forces then the armature is lifted, i.e. it is attracted magnetically by the coil frame. If the current through the coil is switched off than the armature is released for braking.

Material used for armature and coil frame is steel C10, C15 and grey cast-iron GGG40. Their relative permeability μ_r depends strongly upon the grade of saturations and varies in a wide range from 50 up to approximately 1.100. Figure 2 shows the magnetization characteristics for steel C10 and grey cast-iron GGG40.

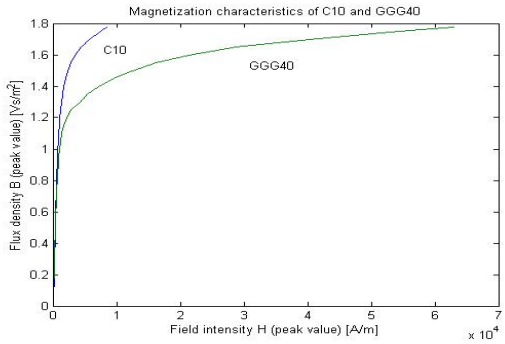

Figure 2: Normal magnetization characteristics of steel C10 and grey cast-iron GGG40 [1]

The mass of the armature is in the range from 100g up to 10kg. Spring forces vary from 100 N up to 12,000 N. The springs are prestressed and can show different characteristics. The air gap varies between 0.2 – 0.7 mm.
The power of the coil is up to 150W and the supply voltage is up to 48V dc from a DC source or up to 207 V dc over a bridge rectifier from the mains.

2. Mathematical modeling

2.1 Equivalent model

Figure 3 represents a sectional view of the brake explaining the basic working principle. The armature is exposed to the magnetic force F_m and the spring force F_{sp}. Sliding friction caused by the moving armature along the guiding bolts is neglected.
The cross-sectional areas A_{F1}, A_{F2} and A_{F3} in [m^2] are all different, whereas $A_{g1} = A_{F1}$ and $A_{g2} = A_{F2}$. The two legs 1 and 2 are equal in length, i.e. $l_{F1} = l_{F2}$ in

[m], and the thicknesses of the bottom sheet (yoke) and the armature are depicted by b_{F3} and b_{A3} in [m].

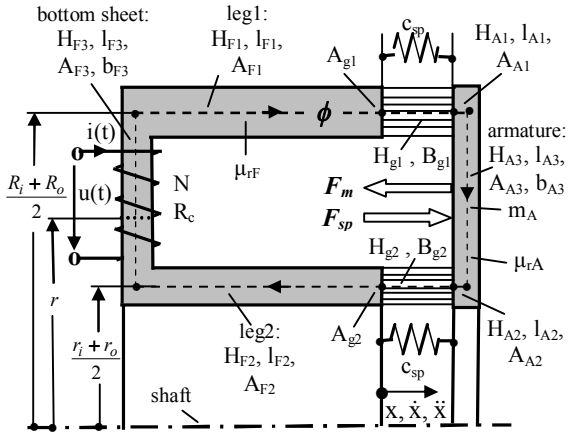

Figure 3: Equivalent model of the brake

The stiffness of the compression springs is represented by the corresponding spring constant c_{sp}. When calculating the magnetic circuit a mean path length for the magnetic flux ϕ in [Wb] is assumed given by the dotted line in Figure 3. Because of the relative high permeability of the magnetic material of the coil frame and the armature the magnetic flux is confined almost entirely to them. Therefore, no leakage fields are considered. In addition, the effect of fringing fields across the air gap is also ignored provided the air-gap length is sufficiently small compared with the dimensions of the adjacent core faces of the coil frame and the armature; this can be assumed tacitly for the given brake system. The cross-sectional areas A_{F1} and A_{F2} are then equal to the cross–sectional areas A_{g1} and A_{g2} of the two air gaps.

2.2 Linear approach

2.2.1 Magnetic flux

Applying ampere's law as [2]

$$\oint \vec{H} \cdot d\vec{l} = Ni \tag{2.1}$$

where

- dl is an element of the magnetic path along the dotted line in Figure 3 as the mean length in [m],
- i is the coil current in [A], and
- N is the number of turns in the coil in [1],

leads to the following relations with the variable x as the actual air gap length in [m] between armature and coil frame:

$$\sum_{3/coil\,frame} H_{Fk} l_{Fk} + \sum_{2/air\,gap} H_{gk} x + \sum_{3/armature} H_{Ak} l_{Ak} = Ni \tag{2.2}$$

Assuming linearity, the magnetic flux density B in [T] and the field intensity H in [A/m] are linked by the magnetic permeability μ in [H/m]

$$\vec{B} = \mu \vec{H} = \mu_0 \mu_r \vec{H} \tag{2.3}$$

where $\mu_0 = 4\pi \cdot 10^{-7}$ H/m is the permeability of free space.

The magnetic flux ϕ crossing a surface S is the surface integral of the normal component of $\vec{B}$, hence

$$\phi = \int_S \vec{B} \cdot d\vec{A} \tag{2.4}$$

If magnetic flux leakage is ignored for simplicity reasons then the flux ϕ is constant along the entire dotted path for a given coil current i. However, the magnetic flux density $\vec{B}$ must change whenever the cross-sections vary.

Introducing the magnetic flux ϕ in equation (2.2) the following expression is obtained:

$$\phi \cdot \left[x\left(\frac{1}{A_{g1}} + \frac{1}{A_{g2}}\right) + \frac{1}{\mu_{rF}}\left(\frac{l_{F1}}{A_{F1}} + \frac{l_{F2}}{A_{F2}} + \frac{1}{2\pi \cdot b_{F3}} ln\frac{R_i + R_o}{r_i + r_o}\right) + \frac{1}{\mu_{rA}}\left(\frac{l_{A1}}{A_{A1}} + \frac{l_{A2}}{A_{A2}} + \frac{1}{2\pi \cdot b_{A3}} ln\frac{R_i + R_o}{r_i + r_o}\right)\right] = \mu_0 Ni \tag{2.5}$$

Considering that the flux link ψ in [Wb] is given by the linear relationship $\psi = N \cdot \phi = L \cdot i$, the inductance L in [H] can be obtained as

$$L(x) = \mu_0 N^2 A_{res} \frac{1}{x + \tau_m \cdot A_{res}} \tag{2.6}$$

with $A_{res} = \dfrac{A_{g1} \cdot A_{g2}}{A_{g1} + A_{g2}}$ (2.7)

and $\tau_m = \dfrac{1}{\mu_{rF}}\left(\dfrac{l_{F1}}{A_{F1}} + \dfrac{l_{F2}}{A_{F2}} + \dfrac{1}{2\pi \cdot b_{F3}} ln\dfrac{R_i + R_o}{r_i + r_o}\right) + \dfrac{1}{\mu_{rA}}\left(\dfrac{l_{A1}}{A_{A1}} + \dfrac{l_{A2}}{A_{A2}} + \dfrac{1}{2\pi \cdot b_{A3}} ln\dfrac{R_i + R_o}{r_i + r_o}\right)$. (2.8)

Rewriting equation (2.6) by substituting

$$k_L = \mu_0 N^2 A_{res} \quad \text{and} \quad d_m = \tau_m A_{res} \tag{2.9}$$

yields the magnetic flux ϕ as

$$\phi(i,x) = \frac{L(x)}{N} i = \frac{k_L}{N} \cdot \frac{1}{x + d_m} \cdot i \tag{2.10}$$

and the magnetic flux link ψ as

$$\psi(i,x) = \phi(i,x) N \tag{2.11}$$

The magnetic flux in equation (2.10) reaches its maximum for a given coil current i at x equal zero, i.e. when the armature is attracted.

Then, $\phi_{max}(i,0)$ depends upon the length d_m which contains the characteristics of the magnet material indicated by the permeability μ_{rF} and μ_{rA} of the coil frame and the armature. They are not constant but a nonlinear function of the flux density $\vec{B}$ and thus varying with the air gap length. Even the permeabilities μ_{rF} and μ_{rA} within the coil frame and the armature differ because of their different cross sections and thus, flux density $\vec{B}$.

2.2.2 Magnetic force

The magnetic force F_m for the brake with two air gaps is calculated with formula (2.12) as [2]

$$F_m = \frac{A_{g1}}{2\mu_0} \cdot B_{g1}^2 + \frac{A_{g2}}{2\mu_0} \cdot B_{g2}^2 \quad . \tag{2.12}$$

With $\phi = B_g \cdot A_g$ the magnetic force is defined as

$$F_m = \frac{\phi^2}{2\mu_0} \cdot \left(\frac{1}{A_{g1}} + \frac{1}{A_{g2}} \right) = \frac{\phi^2}{2\mu_0} \cdot \frac{1}{A_{res}} \quad . \tag{2.13}$$

Inserting the flux ϕ(i, x) from equation (2.10) yields

$$F_m(i,x) = \frac{k_L}{2} \cdot \frac{i^2}{(x + d_m)^2} \quad . \tag{2.14}$$

For air gap x = 0 the magnetic force $\boldsymbol{F_m = F_{m\,max}}$ which depends on the coil current *i* and the length d_m. As long as the current *i* is relatively small, equation (2.14) is suitable to determine the magnetic force F_m and $\boldsymbol{F_{m\,max}}$ in particular correctly. With increasing current i however, the magnetization characteristics in Figure 2 flattens out due to saturation effects and the relative permeabilities μ_{rF} and $\mu_{r\mathrm{A}}$ of the coil frame and armature decrease strongly. As a result, the length *dm* in equation (2.9) changes remarkably to smaller values and the calculation of the magnetic force F_m with equation (2.14) is becoming more and more incorrect.

2.3 Nonlinear approach

2.3.1 Simulation of magnetic flux

The nonlinear relationship of the magnetic flux ϕ as a function of the coil current i and the air-gap x, i.e. ϕ = ϕ(i, x) will be determined in an iterative procedure. Assuming that no leakage of the magnetic flux is considered then ϕ(i, x) is equal in all different parts of along the dotted line of the magnetic circuit according to Figure 3. The iteration is based on Ampere's law given in equation (2.2). Since there is no direct access to the different unknown field intensities H in the coil frame, air gap and armature, the calculation starts from the common magnetic flux and proceeds after the following pattern:

1.) Start with a given initial magnetic flux ϕ(i,x);
2.) Calculate the flux densities B in the different cross sections along the magnetic path;
3.) Determine the field intensities H by including the nonlinear B–H magnetization characteristics of the different material according to Figure 2;
4.) Compare the left side of equation (2.2) with the magneto-motive force (mmf) Ni on the right side. If the difference is less than a pre-given limit then stop the iteration; otherwise continue to the start with an improved value of the magnetic flux ϕ(i, x).

The iteration is carried out for the coil current i = 0 up to the rated current i = i_r, and the air gap x = 0 up to the maximum air gap x = x_g. At the end of the iteration the magnetic flux ϕ(i,x), the magnetic flux densities *B*(i,x) and the magnetic field intensities *H*(i, x) are given along the magnetic path, i.e. the dotted line in Figure 3.

2.3.2 Simulation of magnetic force

The magnetic force F_m is given as [2]

$$F_m = -\left. \frac{\partial W_m(\psi, x)}{\partial x} \right|_{\psi} \tag{2.15}$$

where $W_m(\psi, x)$ is the stored magnetic energy. Mathematically, it is a state function and is obtained from the integral

$$W_m = \int_0^{\psi} i(\psi', x)\, d\psi' \tag{2.16}$$

Since the coil current i as a function of the magnetic flux link ψ and the displacement x of the armature in the air gap is not available directly, the magnetic force F_m is determined by the *coenergy method*. The coenergy $\boldsymbol{W_m^*}$ is defined as a function of i and x from the integral

$$W_m^*(i,x) = \int_0^{i} \psi(i', x)\, di' \tag{2.17}$$

which is also a state function. Hence, the magnetic force F_m can be found as

$$F_m = \left. \frac{\partial W_m^*(i,x)}{\partial x} \right|_{i} \tag{2.18}$$

With the known magnetic flux link ψ(i,x) which is calculated by the iteration procedure explained in section 2.3.1, the magnetic force F_m can be determined by treating and solving equation (2.17) and (2.18).

3. Example

The developed software tools were tested at a brake system with a rated power of 19.17 W. Material for the coil frame is steel C15 and for the armature steel C10.

Essential parameters are [1]:

Rated voltage	24 V
Rated current	0.799 A
Coil resistance	30.1 Ω
Air gap	0.2 mm
Rated spring force	190 N
Mass of the armature	0.074 kg

Simulations were carried out with the software tool MATLAB [3].

3.1 Results of the linear approach

Figure 4 shows the magnetic flux ϕ(i,x) calculated with the linear approach given in equation (2.10).

The unknown permeabilities μ_{rF} and $\mu_{r\mathrm{A}}$ are considered as constant with average values of μ_{rF} = 417 and $\mu_{r\mathrm{A}}$ = 255. With increasing coil current i the magnetic flux ϕ(i,x) increases linearly, too even at air gap length x = 0 which is rather unrealistic.

The magnetic force F_m represented in Figure 5 can be calculated according to equation (2.14) sufficiently correct as long as the air gap length x is not too close to zero. At x = 0 and with growing coil currents the values for F_m become increasingly useless.

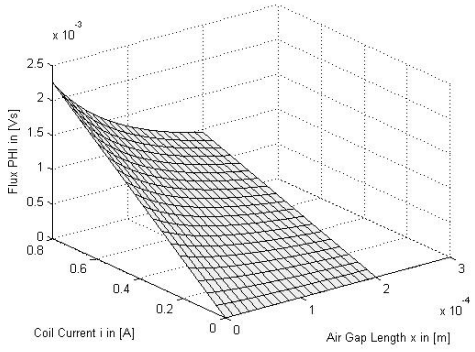

Figure 4: Linear related magnetic flux ϕ(i,x)

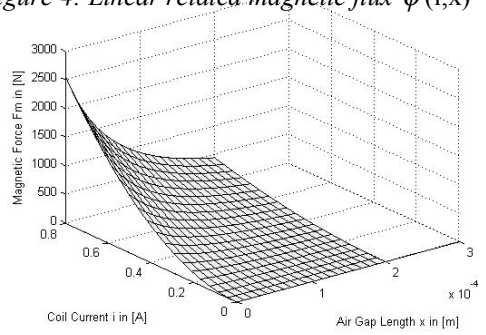

Figure 5: Magnetic force F_m(i,x) calculated with the linear approach

3.2 Results of the nonlinear approach

The given brake system operates deeply in the saturation even at low coil currents as represented in Figure 6. The result differs remarkably compared with the linear approach in Figure 4.

The magnetic force $F_m(i,x)$ shown in Figure 7 which is calculated with equation (2.18) is getting into a high saturation if only the coil current is increased very moderately. It indicates that the results in Figure 5 are only reliable to some extent if the air gap is large enough. Measurements which were carried out at a brake with the specifications given above show a good correspondence with the simulation results. The armature is attracted at an air gap of 0.2 mm with a current of 297 mA which develops a magnetic force of 190 N equal to the rated spring force. The simulation yields 265 mA for this magnetic force.

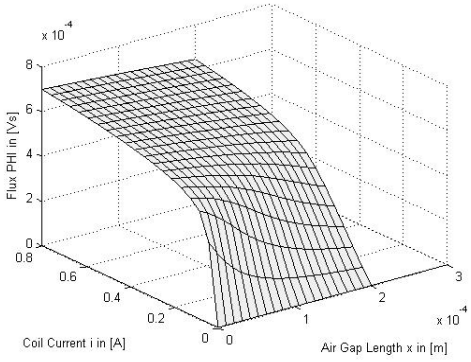

Figure 6: Nonlinear related magnetic flux ϕ(i,x)

The armature is released with a current of 52 mA. From the simulation a value of 61 mA is obtained. Of course, the accuracy of the simulation results can be improved by applying higher number of grids for the numeric calculations.

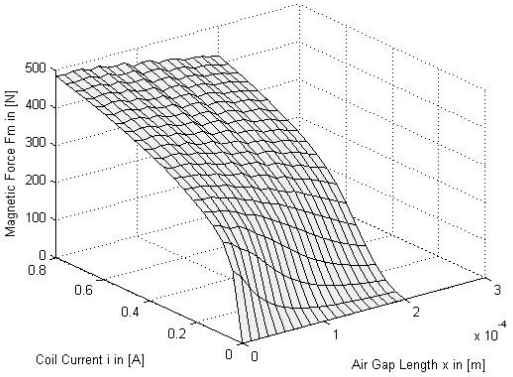

Figure 7: Magnetic force F_m(i,x) calculated with the nonlinear approach

4. Conclusion

The nonlinear effects of the magnetic material in electromagnetic brakes cannot be ignored and the assumption of an average value of magnetic permeability for the material which is accepted in many engineering applications to calculate linearly a corresponding average magnetic force or even semi-empirical correction methods are not satisfying and not reasonable either. The developed simulation software using the nonlinear approach with the coenergy method is a suitable tool to determine the nonlinear relationships of magnetic quantities in electromagnetic brakes. The results are valuable for the efficient design of electromagnetic brakes as for magnetic material, construction characteristic, etc. In addition, they serve for continuing investigation of the brake's dynamic performance [4], [5].

5. References

[1] Chr. Mayr GmbH + Co. KG: www.mayr.de

[2] A.E.Fitzgerald, Ch. Kingsley, St. D. Umans: Electric Machinery; 6. edition, McGraw-Hill, 2003

[3] William J. Palm III: Introduction to MATLAB 7 for Engineers; McGraw-Hill, 2005

[4] P. Poommipech, B. Chukaew: Investigation of the speed dynamics of electromagnetic brakes; senior project; Faculty of Engineering, Department of Electrical Engineering, Thammasat University, 2005; Thailand

[5] J. Steinbrunn: Sensorless Speed Control of Electromagnetic Brakes; EECON-28, 20-21 October 2005; Phuket, Thailand